Agricultural and Forest Meteorology 260–261 (2018) 31–40

Contents lists available at ScienceDirect

Agricultural and Forest Meteorology

journal homepage: www.elsevier.com/locate/agrformet

Impacts of recent climate extremes on spring phenology in arid-mountain ecosystems in China

Zhibin He[a,b,*], Jun Du[a,b], Longfei Chen[a,b], Xi Zhu[a,b,c], Pengfei Lin[a,b,c], Minmin Zhao[a,b,c], Shu Fang[a,b,c]

[a] Linze Inland River Basin Research Station, Chinese Ecosystem Research Network, China
[b] Key Laboratory of Ecohydrology and Inland River Basin, Northwest Institute of Eco-Environment and Resources, Chinese Academy of Sciences, Lanzhou 730000, China
[c] University of Chinese Academy of Sciences, Beijing 100049, China

ARTICLE INFO

Keywords:
Spring phenology
Drought
Warming
Arid mountain ecosystems

ABSTRACT

Phenological responses of terrestrial ecosystems to climate extremes are of growing concern due to the increasing frequency and intensity of extreme climatic events associated with climate change which will in turn affect vegetation seasonality more than gradual changes. However, studies are rare in arid mountain regions where plant development is commonly regulated by both temperature and precipitation. To better understand how arid mountain (AM) ecosystems may respond to climate anomalies, we identified recent extreme climatic events (including intense warming, severe drought, and excessive wetness), and analyzed spring onset of vegetation growth in the Qilian Mountains of northwestern China. Phenological sensitivity was assessed from satellite-based data as departures from maps displaying mean onsets of growth for years 1983–2013. Our results revealed remarkable shifts in the start date of the growing season (SOS) under climate extremes, with different responses depending on ecosystem and altitude. Recent warming induced a general advancement of SOS. Higher spring temperatures enhanced the accumulation of heat needed for budburst and leaf expansion; elevated winter temperatures reduced the chilling days before bud dormancy release, significantly decreasing the risk of freezing injury in AM plants. Changes in SOS observed in this study suggested that AM plants may have relatively low chilling requirement for dormancy release. Contrary to warming, a drought resulted in a widespread delay in spring phenology, with sensitivity peaking over a shrubland ecosystem at medium elevations. This result demonstrated that subalpine shrubs were most susceptible of the studied ecosystems to hydroclimatic extremes, highlighting the great importance in this biome of concerns. Moreover, during the year when multiple extreme events (e.g. intense warming and heavy rainfall) coincided, their combined influence appeared to arise from synergistic mechanisms that are in urgent need of further research.

1. Introduction

Climate change places the structural and functional stability of terrestrial ecosystems at risk, with possible effects on the patterns of biogeographical distribution, interactions with the physical environment, and on species diversity and persistence (Walther et al., 2002; Parmesan and Yohe, 2003; Heyder et al., 2011). Several studies documented a close coupling of the dynamics of plant growth and animal migration over the past decades with patterns of climate change (Nemani et al., 2003; Thuiller et al., 2005; Richardson et al., 2013). Recent research indicates that extreme climate events increased dramatically in the frequency, intensity, duration, and spatial extent during the course of climate change over the past half century (e.g. Menzel et al., 2011; Butt et al., 2015; Ma et al., 2015). These extreme changes impose a substantial challenge on natural ecosystems because extreme climate may exceed the ability of species to adapt to new conditions through phenotypic plasticity or adaptive evolution, and may result in a decrease in fitness and a potential increase in the risk of local extinctions (Ghalambor et al., 2007; Siegmund et al., 2016).

Vegetation phenology—the timing of annually-recurring growth events—represents a key attribute of ecosystem functioning, and plays an important role in regulating terrestrial biochemical cycles, such as energy exchange, water balance, and carbon sequestration (Badeck et al., 2004; Peñuelas and Filella, 2009; Richardson et al., 2013). Changes in phenology are among the first signals of adjustments in species responses to climate anomalies (Walther et al., 2002), and they have been unequivocally attributed to temperature variation (Menzel et al., 2011; Richardson et al., 2013). Though the evidence for

* Corresponding author.
E-mail address: hzbmail@lzb.ac.cn (Z. He).

https://doi.org/10.1016/j.agrformet.2018.05.022
Received 28 December 2017; Received in revised form 28 May 2018; Accepted 28 May 2018
Available online 06 June 2018
0168-1923/

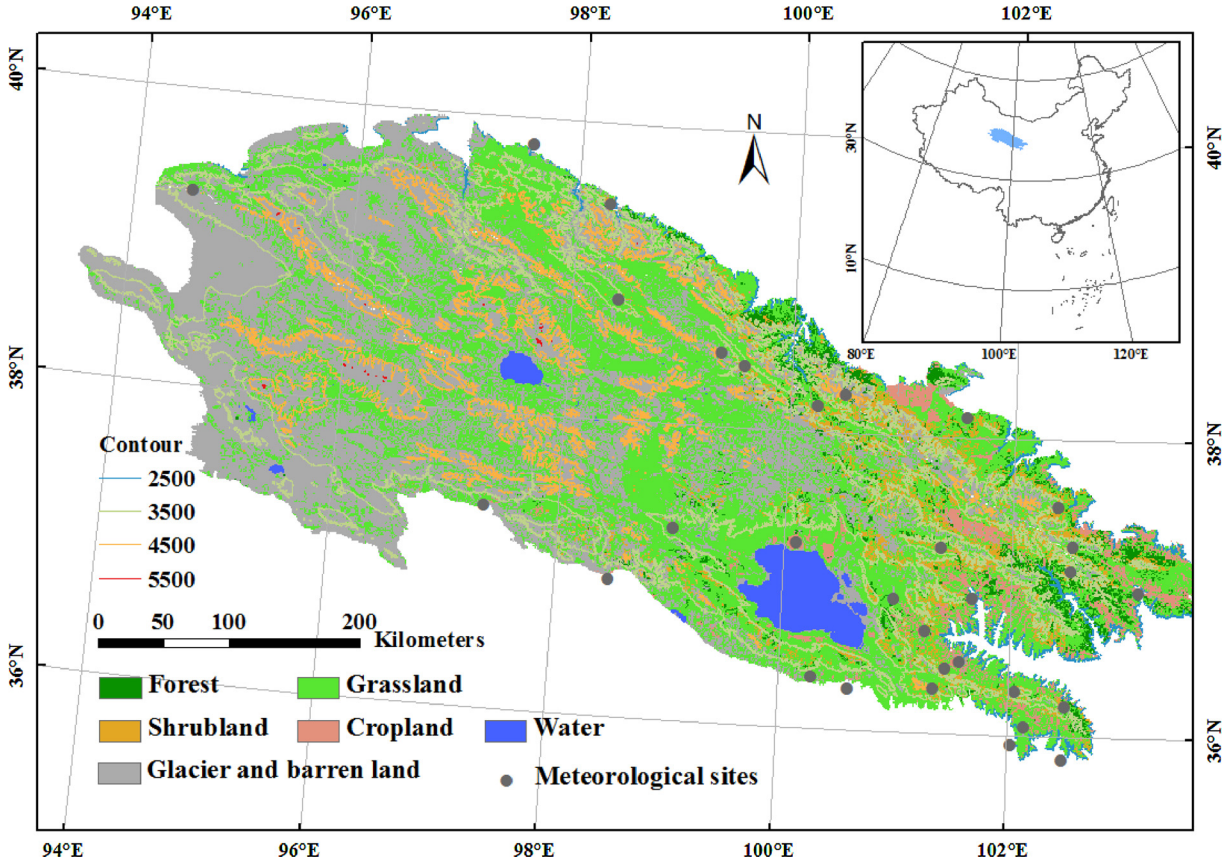

Fig. 1. Location of the Qilian Mountains and spatial distribution of meteorological stations.

phenology-climate relationships is increasing, the magnitude and direction of phenological responses to extreme climate events such as drought and heat spells remain largely uncertain. It is very likely that the seasonal trajectory of vegetation activities is more sensitive to the extremes than to the gradual changes in climate (Butt et al., 2015; Crabbe et al., 2016; Siegmund et al., 2016). During droughts, for example, severely-delayed or even undetectable phenological cycles were noted in dryland ecosystems in Australia (Ma et al., 2015). Indeed, phenological responses to climate extremes can be diverse and highly complex, and vary with the type of event, across regions, and among biomes. In a recent study of four shrub species in Germany, authors found a generally strong negative effect of temperature on flowering, but hardly any systematic influence of increased spring rainfall (Siegmund et al., 2016). In a mixed woody-herbaceous ecosystem, Rich et al. (2008) observed that herbaceous plants responded to a drought event faster, and tracked optimal growing conditions more closely than did woody plants. Across different climatic zones from northeastern to southeastern China, Zhang and Tao (2013) simulated changes in rice phenology, and reported that the rice growing season under extreme temperatures would decrease by up to 6 days at the national scale, but varied regionally, and in fact exhibited an opposite trend in the northeast. These findings highlight the imperative need to develop a greater knowledge of climatic controls on vegetation phenology, especially of the effects of extreme events on species in regions that are infinitely sensitive to climate change.

Arid mountains (AMs) constitute a special geomorphic unit that develops in arid/semi-arid climate zones at high altitudes. The environmental components are affected by the climate type of baseband, and exhibit characteristics of vertical zonality. AMs normally act as islands of biodiversity in relatively barren areas, and are rich in rivers that nourish piedmont oases and natural plants (Diaz et al., 2003). Because of high heterogeneity in landscape types, AMs have long been regarded among the most fragile environments in the world (Nogués-Bravo et al., 2007). Biomes in the AMs are undergoing profound changes due to recent climate anomalies (Beniston, 2003; Crimmins et al., 2010; He et al., 2015). In particular, alterations in the temporal niche of vegetation phenophases caused a significant concern among ecologists (Lesica and Kittelson, 2010; Du et al., 2014; Prevéy and Seastedt, 2014; Zhou et al., 2016). Additionally, the magnitude of climate change in the northern-latitude mountains including AMs is often greater than that in other natural systems (Nogués-Bravo et al., 2007). In China, northwest inland AMs experienced a rapid temperature rise of 0.26 °C per decade during the past 50 years, higher than the national rate of 0.14 °C/decade (Du et al., 2014). More importantly, ongoing occurrences of many types of climatic extremes, such as heavy rains and high nighttime temperatures, have become extraordinarily frequent (Lin et al., 2017). Extreme winter warming has also been observed recently, conditions that were rare or unprecedented in early climatological records (Lin et al., 2017). With abrupt warming, the timing of leaf-unfolding in subalpine shrubs in the AMs exhibited a significant trend toward earlier dates, at about 3.7–4.9 days per decade (He et al., 2015). Changes in ecological functioning of AMs are thought to be closely associated with extreme climate events, indicating great uncertainty in the role of arid mountain ecosystems in regional carbon cycling.

Two of the most critical climate variables regulating phenological dynamics of AM plants involve temperature and precipitation; vegetation activity at high altitudes is often affected by temperature variability, while plant growth in lowlands tends to be limited by water stress (Crimmins et al., 2010). The interaction between temperature and precipitation compounds the difficulty with understanding the mechanism of phenological responses (Lesica and Kittelson, 2010). In addition, snowmelt in some high-altitude ecoregions such as the Tibetan Plateau, where snow accounts for most of the precipitation (Wang et al., 2013), often provides an important supplemental water source,

and thus exerts an influence on the phenological development of low-growing vegetation (Julitta et al., 2014). Nonetheless, vegetation growth in the AMs is thought to be less sensitive to snow cover due to the thin snowpack in winter (mean snow depth < 5 mm, Peng et al., 2010), and fast melting over a short period of time (Dorji et al., 2013). Thus, extreme events in the AMs associated with temperature and precipitation include droughts, rainstorms, heat waves, cold spells, and their combinations. The implications of these climate extremes for AM plants are still not clear (Crimmins et al., 2010). To predict possible responses of AM ecosystems under a changeable climate in the future, we investigated the influence of recent extremely high temperature, heavy rainfall, and severe drought on spring phenology of diverse biomes in the arid mountains of China. Results of this study will permit more accurate ecological modeling of carbon cycles in a future changing world.

2. Materials and methods

2.1. Study area

This study focuses on the Qilian Mountains (QLMs) in northwestern China. The QLMs span a latitudinal range of 35.8–40.0 °N and longitudinal extent of 93.5–104.0 °E, covering 1.93×10^5 km^2 (Fig. 1). As one of the major arid mountains in China, QLMs border the northern margin of the Tibetan Plateau and southern limits of Badain Jaran and Tengger Deserts; they are traversed by the Hexi River Corridor oasis in the piedmont areas. Vegetation in the QLMs plays a major role in fostering and regulating water resources, and its dynamics has an important influence on regional ecological stability. Climate across the QLMs is characteristic of temperate continental plateaus, in that it is cool and arid (Du et al., 2014). The mean annual temperature for a 34-year period (1982–2015) was 4.1 °C, and annual cumulative precipitation was 340 mm. About 90% of the precipitation falls as rain, and is concentrated in May to September; this results in low snowfall in winter (Bourque and Mir, 2012). Snow is mainly found in non-vegetated regions above 4500 m above sea level (a.s.l.) (Jiang et al., 2016, Fig. 1). Temperature is commonly above 0° starting at the end of March, and snow cover melts over a short period of time due to the high insulation (Dorji et al., 2013). Spatial heterogeneity of climatic conditions determines the distribution of vegetation.

Vegetation in the QLMs can be classified into four land cover types: forest, shrub, grass, and cropland. The forest is dominated by Qinghai spruce (*Picea crassifolia*), and mainly distributed in the northern and eastern part of the QLMs, at a mean altitude of 3160 m (a.s.l.) (Table 1). Shrubland is primarily located in the subalpine zones of the QLMs above the treeline. Common shrub species are *Salix gilashanica*, *Caragana jubata*, and *Potentilla fruticosa* (He et al., 2015). Grassland has a wide geographical distribution at altitudes ranging from 2500 to 4600 m. Several constructive species, such as *Stellera chamaejasme Linn.* and *Potentilla multifida*, are also present, collectively covering 42.4% of the area.

2.2. Data

2.2.1. Meteorological data

We used daily climatic observations for the period of 1982–2013 from the China Meteorological Data Service Center of the China Meteorological Administration (http://cdc.cma.gov.cn) for analyses of extreme events. The meteorological data set included daily mean temperature (T_{mean}), daily maximum temperature (T_{max}), daily minimum temperature (T_{min}) and precipitation (P), and was derived from 26 national meteorological stations across the QLMs as well as 5 stations in the immediate vicinity of the boundary (Fig. 1 and Table 2). These stations cover the distribution ranges of the studied vegetation biomes.

2.2.2. Land cover map

We used a 1:100,000 raster map of vegetation types, created by the Chinese Academy of Sciences (http://westdc.westgis.ac.cn), to classify different land covers in the QLMs. This land cover data set has a high accuracy because it maximizes the retention of real information (He et al., 2015). Seven dominant vegetation biomes were identified, including closed forest, open forest, brushwood, shrubland, meadow, steppe, and cropland. We then assigned each biome to one of the following functional types: forest, shrub, or grass (see Table 1 for details). The cropland was not considered in the study because of extensive human intervention.

2.2.3. MODIS NDVI

The Normalized Differential Vegetation Index (NDVI), based on the differential reflectance of green vegetation in the infrared and near-infrared bands, has been successfully used as an indicator of plant canopy greenness and productivity, because it is strongly related to the strength of photosynthetic activity (Pettorelli et al., 2005; Jeong et al., 2011). In this study, we used a MODIS (Moderate-resolution Imaging Spectro-radiometer) NDVI dataset spanning the period from February 2000 to December 2013 to retrieve the starting date of the vegetation growing season (SOS) across the QLMs. The 16-day maximum-value composite MODIS NDVI data (product MOD13A2) at a spatial resolution of 1 km were generated from atmospherically-corrected bi-directional surface reflectances that had been masked for water, clouds, heavy aerosols, and cloud shadows (Zhang et al., 2013), and obtained through the online Data Pool at the NASA Land Processes Distributed Active Archive Center (LPDAAC) (http://LPDAAC.usgs.gov). This dataset has been widely used and tested in the retrieval of remote-sensing phenology across diverse vegetation biomes and in different climatic regions, and their robustness for SOS trend analyses were validated (Zhang et al., 2004; Delbart et al., 2006; Kross et al., 2011). For extracting NDVI data for the areas of interest (forest, shrubland and grassland), the land cover map mask was used. Subsequently, pixels showing the annual mean NDVI of < 0.1 were removed to improve the accuracy of the analysis in case of possible uncertainties in the land cover map and vegetation changes (Jeong et al., 2011).

2.3. Methods

2.3.1. Definition of climate extremes

Extreme climate events are often reflected in temperature and

Table 1
Summary of major land cover types in the Qilian Mountains.

Type	Area (km^2)	Percentage of total area (%)	Altitude of distribution (m)	Dominant species	Composition
Forest	6190	3.2	3160 (2547–3926)[a]	*Picea crassifolia*	closed forest, open forest
Shrub	9966	5.2	3425 (2806–4045)[a]	*Salix gilashanica, Caragana jubata, Potentilla fruticosa*	brushwood, shrubland
Grass	81811	42.4	3604 (2581–4626)[a]	*Stellera chamaejasme Linn., Potentilla multifida, Agropyron cristatum Gaertn., Artemisia annua Linn., Iris ensata*	meadow, steppe

Note: [a] 95% confidence interval for distribution altitudes is given in parentheses.

Table 2
Site characteristics of meteorological stations.

Station	Altitude(m)	Coordinates	Annual mean temperature (°C)	Annual total precipitation (mm)
Juquan	1477	39°28' N, 94°17' E	7.9	88
Wuwei	1532	37°33' N, 102°24' E	8.8	174
Minhe	1814	36°12' N, 102°30' E	8.4	338
Xunhua	1883	35°51' N, 102°29' E	9.1	272
Yongchang	1977	38°08' N, 101°35' E	5.6	215
Jiazha	2057	35°56' N, 102°02' E	8.4	348
Gulang	2072	37°17' N, 102°32' E	5.9	353
Pingan	2125	36°18' N, 102°04' E	7.4	335
Subei	2137	39°19' N, 94°31' E	7.2	156
Yumen	2259	39°49' N, 97°34' E	7.6	69
Minle	2281	38°15' N, 100°30' E	4.2	347
Xining	2295	36°26' N, 101°27' E	6.1	400
Sunan	2312	38°30' N, 99°22' E	4.3	258
Huzhu	2480	36°30' N, 101°35' E	4.2	502
Tianzhu	2497	36°59' N, 103°07' E	3.1	361
Datong	2587	36°55' N, 101°41' E	4.4	525
Huangzhong	2649	36°30' N, 101°34' E	4.4	541
Huangyuan	2670	36°41' N, 101°16' E	3.6	421
Qilian	2787	38°11' N, 100°15' E	1.5	421
Hualong	2835	36°04' N, 102°09' E	2.9	456
Gonghe	2849	36°17' N, 100°37' E	4.7	321
Wulan	2970	36°56' N, 98°29' E	4.2	216
Menyuan	2979	37°15' N, 101°23' E	1.4	524
Delingha	2991	37°22' N, 97°22' E	4.5	203
Haiyan	3017	36°54' N, 100°59' E	1	407
Wushaoling	3045	37°07' N, 102°31' E	0.5	413
Tuole	3144	38°49' N, 98°25' E	−2.1	314
Yeniugou	3180	38°25' N, 99°36' E	−2.5	432
Qinghaihu	3202	36°21' N, 100°18' E	0.8	430
Gangcha	3236	37°15' N, 100°07' E	0.2	395
Tianjun	3409	37°18' N, 99°01' E	−0.6	365

precipitation anomalies that are rare, severe, and unique compared to the average conditions over a certain period of time (Menzel et al., 2011; Butt et al., 2015). In this study, we focused on yearly events including extremely high temperature (warm), heavy rainfall (wet), and severe drought (dry) that occurred from 2000 to 2013 across the QLMs. This analysis did not take into account cold-temperature extremes because detection of extremely cold events was much more difficult during the period of our study compared to the long-term climate trajectory as a result of climate warming (Lin et al., 2017). Before classifying climate anomalies, we analyzed available daily climatological records for each station for years between 1983 and 2013 to determine annual temperature and precipitation means. Taking into account any chilling requirement that may have affected phenology, a year was assigned from 1st of September of the year prior to SOS to 31st of August of current SOS. This also accounted for lag effects of climate on phenology; lag effects of climatic conditions in preceding autumn and winter on the spring onset of growth were widely reported (Nordli et al., 2008; Yu et al., 2010; He et al., 2015). Then, we calculated the annual climatological departures for all meteorological stations according to Eq. (1):

$$D_j = \frac{\sum (X_{i,j} - \overline{X_i})}{n} \quad (1)$$

where D_j was the climatological departure in year j, $X_{i,j}$ was the annual temperature/precipitation at station i in year j, $\overline{X_i}$ was the mean value from 1983 to 2013 at station i, and n was the number of stations. Climatological observations that fell outside of the 20th and 80th percentile of the yearly departure time series were identified as extremes (Fig. 2). We then filtered these extremes using the following criteria (Table S1) based on the inter-annual variability of temperature and precipitation: (1) in the warm year, D_j of precipitation was as close to the historical mean value as possible when the yearly temperatures (including T_{mean}, T_{min}, and T_{max}) exceeded the 80th percentile of the departure time series; (2) in the wet (or dry) years, D_j of temperatures was as close to the historical mean values as possible when annual precipitation exceeded the 80th percentile (or fell below the 20th percentile) of the departure time series; (3) in the warm and wet year, all climatic observations needed to fall in the upper 20th percentile of the probability distribution for departures; (4) in the normal year, D_j of temperature and precipitation was as close to the historical mean values as possible; (5) for all events, the standard deviation of D_j for stations of each climatic observation was reduced to an absolute value of the minimum. After data screening using these control conditions, we ultimately focused on a normal event in 2003, a warm event in 2010, a wet event in 2012, a dry event in 2001, and a warm and wet event in 2009 (Fig. 2 and Table 3). To further test the applicability of the selected normal year, we compared SOS in 2003 with the mean values during 2000 to 2013. Results of the small difference in mean SOS and the approximate normal distribution of SOS anomaly confirmed the rationality of our screening methods (Fig. S2).

2.3.2. Retrieval of remote sensing SOS

Before retrieval of remote sensing SOS, preprocessing procedures are necessary with NDVI time series. First, we eliminated the effect of snow cover on NDVI for each pixel; snow cover in winter and early-spring often depresses NDVI values, leading to possible biases in determining seasonality in vegetation greenness (Delbart et al., 2006). With the support of the flag file (snow free records from MOD13A2 dataset) for data quality, we identified pixels where snow cover possibly existed, and interpolated values by the spline method on the basis of uncontaminated pixels. If negative outliers in the time series remained, we further applied the median-filter method for each pixel using the nearest-interpolation algorithm. Subsequently, clouds and poor atmospheric conditions in the course of vegetative growth can also result in abnormally high/low NDVI values. To remove these spikes from the NDVI ascending periods, we used the Savitzky-Golay filter with a five-point moving window with each NDVI cycle, as in previous studies (e.g. Shen et al., 2015). Finally, a logistic model was employed

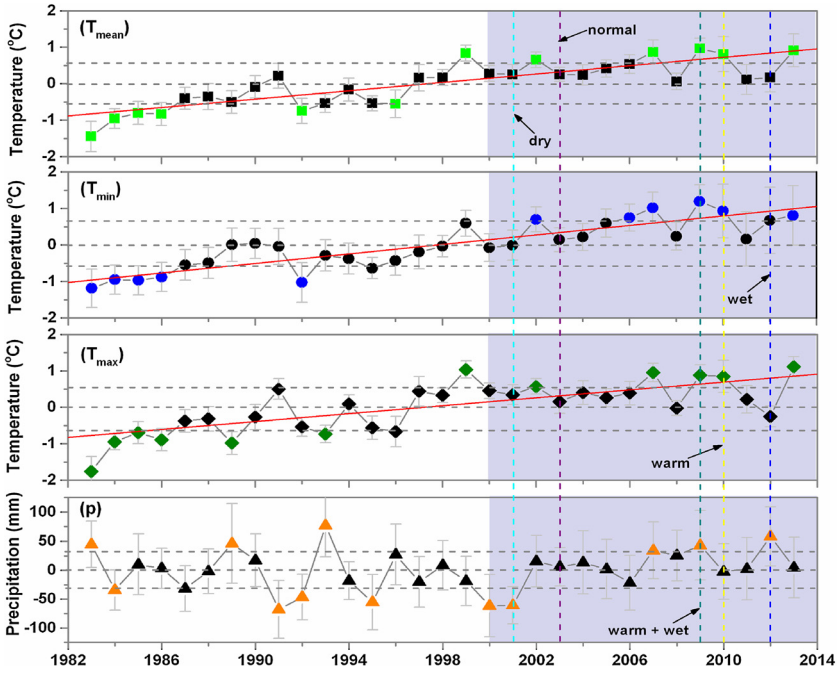

Fig. 2. Climatology (T_{mean} in squares, T_{min} in circles, T_{max} in diamonds, and P in triangles) of the Qilian Mountains from 1983 to 2013. Plotted data are mean climatological departures. The error bar shows the standard error of the mean. Modeled climate changes are depicted by a single red solid trend line. Climatic observations that fell outside the 20th (top dashed line) and 80th (bottom dashed line) percentile of the yearly departure time series were identified as extremes (the colored points). The colored vertical lines represent the years of extreme and normal climate. For interpretation of the references to colour in this figure legend, the reader is referred to the web version of this article.

to fit the temporal variation of the filtered NDVI data for an annual growth phase. The logistic model function has the form (Zhang et al., 2004):

$$y(t) = \frac{c}{1 + e^{a+bt}} + d \tag{2}$$

where $y(t)$ was NDVI at time t, parameters a and b controlled the shape of the curve, c and d determined the amplitude values in a single year, and d represented the initial background NDVI value. After that, the date of vegetation SOS was retrieved from pre-processed NDVI data using the inflection point-based method (RC_{max}), which has been described and tested in diverse biomes in different climatic zones, and validated for robustness in extracting phenological metrics (Zhang et al., 2004; Shen et al., 2015). The RC_{max} method is based on the rate of change (RC) of the fitted NDVI curve, which is the derivative of the curvature calculated with Eq. (3):

$$RC = b^3 cz\left\{\frac{3z(1-z)(1+z)^3[2(1+z)^3 + b^2c^2z]}{[(1+z)^4 + (bcz)^2]^{\frac{5}{2}}} - \frac{(1+z)^2(1+2z-5z^2)}{[(1+z)^4 + (bcz)^2]^{\frac{3}{2}}}\right\} \tag{3}$$

where $z = e^{a+bt}$, and a,b, and c were as in Eq. (2). We then defined the date of SOS as the time when the rate of curvature-change achieved the first local maximum.

2.3.3. Statistical analysis

We obtained the altitudinal distribution range for each vegetation type (forest, shrub, and grass) by overlaying the land cover map with digital elevation model (DEM) data. Within individual event years, climatic statistics were also conducted during phenologically-relevant periods. As the length of the phenologically-relevant period for temperature and precipitation could vary among vegetation types, we did

Table 3
Summary of climatology for individual event years, and long-term means for 1983–2013. Different phenologically-relevant periods for the three ecosystems were used, according to PLS regressions.

Year	Sep.(previous year)–Aug.(current year)				Nov.–Jan. (previous winter) (Forest)		Mar.–Jun. (current spring) (Forest)	
	T_{mean}(°C)	T_{max}(°C)	T_{min}(°C)	P(mm)	T_{mean}(°C)	P(mm)	T_{mean}(°C)	P(mm)
2003	4.38	11.94	−1.76	362.4	−6.65	7.2	7.40	111.0
2001	4.39	12.12	−1.98	288.4	−6.54	9.6	7.31	76.2
2009	5.11	12.67	−0.78	392.0	−6.01	6.8	8.49	135.9
2010	4.95	12.63	−1.04	346.8	−5.89	7.7	7.62	122.3
2012	4.31	11.53	−1.31	407.2	−7.05	10.5	7.41	158.2
1983–2013	4.14	11.78	−1.98	349.0	−6.96	6.9	7.29	125.0

Nov.–Jan. (previous winter) (Shrub)		Apr.–Jun. (current spring) (Shrub)		Nov.–Jan. (previous winter) (Grass)		Apr.–Jun. (current spring) (Grass)		Event
T_{mean}(°C)	P(mm)	T_{mean}(°C)	P(mm)	T_{mean}(°C)	P(mm)	T_{mean}(°C)	P(mm)	
−6.65	7.2	10.23	102.7	−6.65	7.2	10.23	102.7	Normal
−6.54	9.6	10.20	75.7	−6.54	9.6	10.20	75.7	Dry
−6.01	6.8	11.53	126.9	−6.01	6.8	11.53	126.9	Warm and wet
−5.89	7.7	10.79	112.9	−5.89	7.7	10.79	112.9	Warm
−7.05	10.5	10.29	149.4	−7.05	10.5	10.29	149.4	Wet
−6.96	6.9	10.27	119.4	−6.96	6.9	10.27	119.4	Long-term mean

T_{max}, the maximum air temperature; T_{min}, the minimum air temperature; T_{mean}, the mean air temperature; P, precipitation.

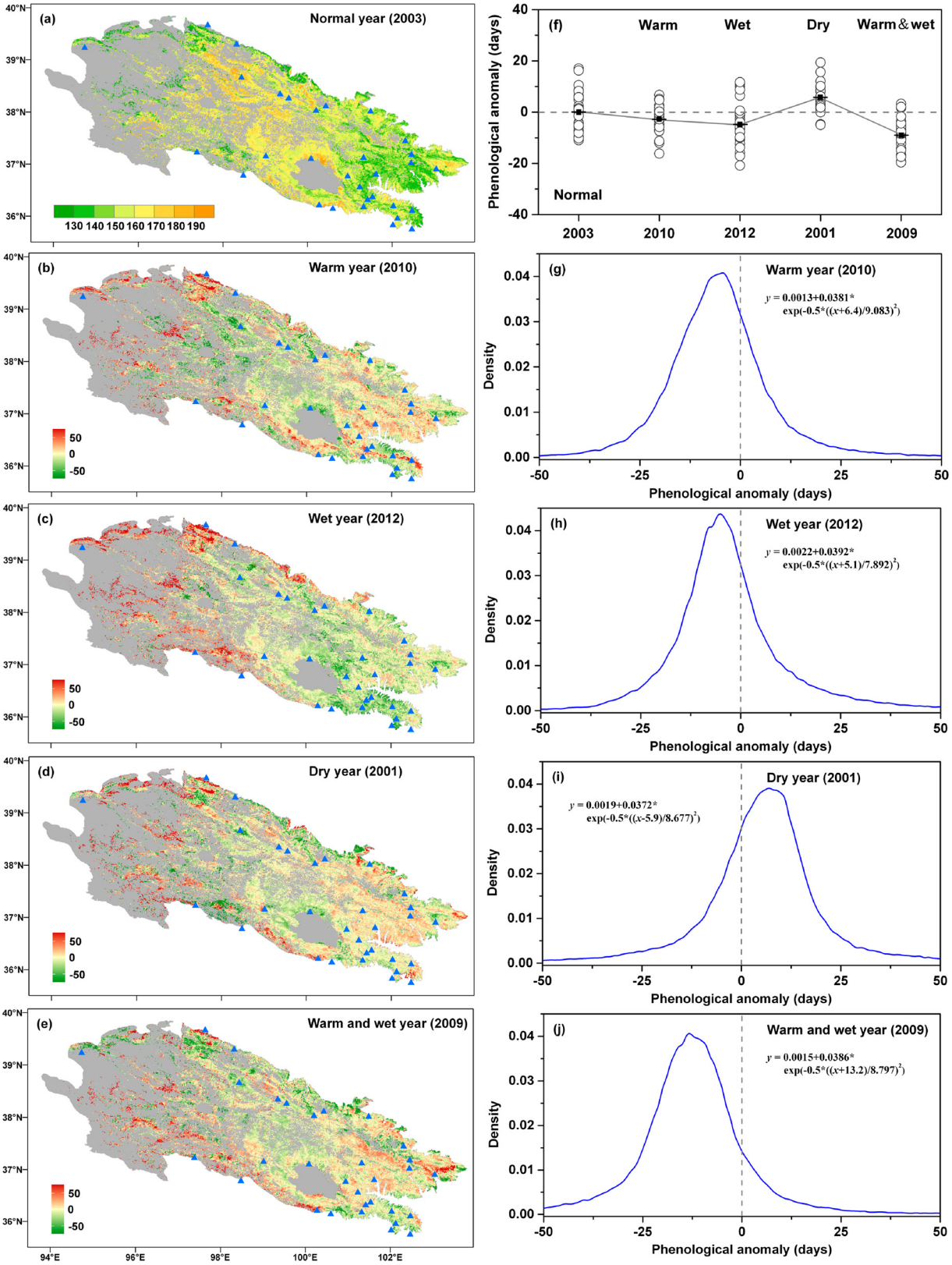

Fig. 3. (a) Spatial distribution of green-up date (Julian day) in the normal year (2003), and differences (i.e. phenological anomaly) in SOS between years with an extreme climate event (b–e) and the normal year. (f) Similar to (b–e), but using phenological data at station-scale. Points represent the average value of pixels around meteorological stations (g–j) Plot of the probability density function for SOS anomaly for individual climate events over the Qilian Mountains. For interpretation of the references to colour in this figure legend, the reader is referred to the web version of this article.

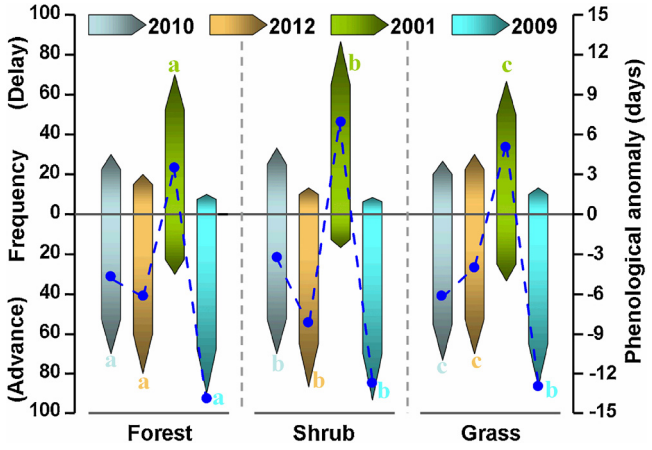

Fig. 4. Comparisons of averages in SOS anomaly (blue dots) under extreme climate events among the three major vegetation types of the Qilian Mountains and the corresponding changes in frequency of SOS anomaly in pixel-level analysis. The differences of averages in SOS anomaly among vegetation types were tested using a *Bonferroni*'s test. For interpretation of the references to colour in this figure legend, the reader is referred to the web version of this article.

not use a fixed period. Instead, the length of the phenologically-relevant period was determined separately with an effective method based on partial least square regression (PLSR, Luedeling and Gassner, 2012). Here, we evaluated phenological responses of the different ecosystems to monthly temperatures, relating datasets by PLSRs. In this analysis, the variable importance plot (VIP) and the regression coefficient were calculated (Fig. S1, Yu et al., 2010). Predictors with a VIP of more than 1.0 were considered important. Accordingly, the phenologically-relevant periods for the three ecosystems were determined. To assess the phenological responses to extreme climate events, we calculated SOS anomalies as SOS_{event} (SOS in the extreme-event year) – SOS_{normal} (SOS in the normal year), with positive and negative differences indicating a delay or advancement in SOS, respectively. We plotted probability distribution of SOS anomaly against the corresponding density function. The magnitude of response of each vegetation type to a climatic event was defined as the mean value and frequency of SOS anomaly. The differences in magnitudes of responses among vegetation types were tested using a *Bonferroni*'s test. Given the uneven spatial distributions of the three ecosystems, the heterogeneous sampling size of total area could bias the results of our analysis. To examine whether or not sampling size had an important influence on phenological responses to extreme climatic events, the above analysis was conducted twice, first on all pixels across the QLMs, and second on only those pixels that represented the 20 km-buffer area around meteorological stations. For the station-level analyses, we averaged the remote sensing SOS of these pixels for individual ecosystems. In addition, to investigate how extreme climate events influenced the altitudinal gradient of SOS, we calculated the average green-up date for every 100 m in altitude, and then fitted a linear regression trend to SOS against altitude.

3. Results

3.1. Recent climate extremes in arid mountains of China

The PLSR showed a clear pattern of significant influences of climatic conditions during different phases (previous winter and following spring) of the dormancy period on SOS in the QLMs. For example, the start of the growing season for grassland was mainly determined by temperatures in November to January, and during April and June (Fig. S1). Changes in temperature and precipitation in these phenologically-relevant periods have been shown to be comparable to, or even exceed, those of the annual statistics (Table 3). Historical yearly records for the period from 1983 to 2013 revealed significant warming trends at a rate of 0.56–0.61 °C per decade ($P < 0.01$), with the most notable warming for T_{min} (Fig. 2). As a result, extensive warm spells dominated in recent years, especially since 2000 (annual temperatures in 19.4% of years exceeded the 80th percentile of the departure time series). These anomalies exhibited a clear tendency toward an increase of spring and winter temperatures (Table 3). In contrast, few or no cold spells (extremely low temperatures) were detected in recent years (Fig. 2). Most of the precipitation in the QLMs is concentrated in spring and summer. Although a noticeable trend in annual precipitation during the past decades was not observed ($P = 0.38$), occurrences of droughts have become less frequent, especially in recent years. For example, during 1982–1999, four droughts were registered in most of meteorological stations across QLMs, while there were only two since the year 2000. In comparison, the frequency of wet events (extremely heavy rainfall) increased during the last decade, and in 2012, the amount of annual precipitation exceeded the historical average by 58.2 mm, 57% of which was concentrated in the preseason period. In view of these characteristics of recent climatic variations in the QLMs, four extreme events were identified with our screening method: a warm event in 2010, a wet event in 2012, a dry event in 2001, and a warm and wet event in 2009. We also defined 2003 as the normal year that paralleled the long-term means (Table 3).

3.2. Phenological impacts of recent climate extremes

SOS anomalies were mapped for each pixel to assess spatial patterns in phenological responses to climate extremes over the QLMs (Fig. 3). In 2010 (the warm year), the majority of pixels (70.3%) exhibited a mean advance of 6.4 days in the green-up date (Fig. 3b and g), especially in the central parts of the distribution range of grasslands. During the precipitation-involved events, we observed a generally-advancing trend in SOS in the wet year ($\Delta SOS = -5.1$ days, Fig. 3h), and a delaying trend in the dry year ($\Delta SOS = 5.9$ days, Fig. 3i). These occurred mainly in the western part of the QLMs, where forests and shrublands dominated the vegetation (Figs. 1 and 3c–d). When increasing temperature co-occurred with increasing rainfall, a more palpable change in SOS was observed, and in 2009, the mean green-up date was shifted by 13.2 days earlier across 86.6% of the study area (Fig. 3e and j). A similar response pattern was also present for SOS anomalies at station-level (Fig. 3f).

This spatial heterogeneity in phenological sensitivity to climate extremes was dependent on geographical distribution of land cover types. A comparison of responses of SOS at ecosystem level (Figs. 4 and S3) revealed that SOS in grassland was more sensitive to warm spells in preseason than the other two biomes in the QLMs. In contrast, the severity of responses to the wet event increased from grassland to shrubland and forest, and peaked over subalpine regions where low shrubs were dominant. The likely reason for this pattern was that the alpine meadows at high altitudes were characterized by cold and wet climate, whereas forests and shrubs occupied the relatively warm and dry low altitudes in the QLMs. With a further investigation of how altitudinal gradient of SOS changed across space during different events, we found that the overall slope of the fitted curve of SOS against altitude across the QLMs decreased during warm and dry years in comparison to the normal year (Fig. 5a). Additionally, we also observed opposite trends in forests and shrubs during the dry year (Fig. 5b), which suggested that these ecosystems have greater sensitivities to water stress in the upper parts of the distribution range. When preseason rainfall was abundant, the altitudinal gradient in SOS increased substantially regardless of vegetation type (Fig. 5b). Changes in altitudinal gradient indicated that spring phenology at high elevations was extremely susceptible to a warming effect, whereas variability in preseason precipitation significantly affected the dynamics of SOS in lowlands. For example, in the 2012-warm (the 2001-dry) year,

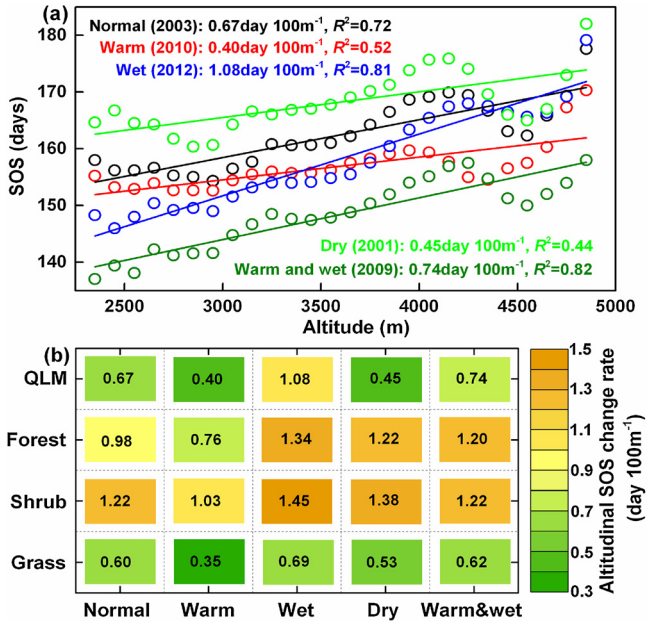

Fig. 5. (a) Altitudinal gradients in the green-up date for the normal year and years with a climate event in the Qilian Mountains. (b) Rate of altitudinal SOS change for the three major vegetation types. QLM means the average for all.

vegetation in the QLMs exhibited an advance in the green-up date of 2.7 days (an delay of 7.4 days) at the altitude of 2500 m, while the timing of SOS was advanced by 8.1 days (delayed by 3.1 days) at the altitude of 4500 m in comparison with the normal year. In addition, it was noteworthy that the pattern of greatest altitudinal gradient in SOS for shrubland remained consistent across events, reflecting the most acute sensitivity to environmental stresses in the QLMs.

4. Discussion

An increased frequency of climatic extremes has added a pivotal uncertainty in predicting future impacts of climate change on ecosystems. There is an urgent need to explore how terrestrial ecosystems, especially those tagged as fragile and susceptible, react to increasing climate change (Ghalambor et al., 2007; Ma et al., 2015; Siegmund et al., 2016). Here, we reported research findings on the influence of recent extreme climate events on spring phenology in several biomes in arid mountains of China using two types of analysis. Our results showed significant changes in SOS under climatic extremes; these changes were ecosystem-specific, and varied with altitude. A similar response pattern was shown with statistics at pixel scale and at station level (Figs. 4 and S3), revealing a minor influence of sampling size on phenological responses to climatic extremes.

We observed an advance in SOS for QLM plants during the extreme warming event (in 2009), and that was consistent with other studies of spring phenology (Menzel et al., 2011; He et al., 2015; Crabbe et al., 2016); the SOS advance in this study was greatest in the grassland ecosystem at the highest average elevations (Fig. 4 and Table 1). Given the clear relations with SOS (Fig. S1), increased temperatures in the winter prior to and during the following spring appear collectively responsible for the observed phenological pattern. Higher spring temperatures enhanced the accumulation of heat needed for budburst and leaf expansion, while elevated winter temperatures reduced the chilling days before bud dormancy release. Other authors attributed temperature effects on the timing of leaf-out in temperate plants to the dynamic relationship between the chilling requirement (sufficient amounts of exposure to cold days) and thermal accumulation (a certain amount of thermal time) (Ghelardini et al., 2010; Polgar and Primack, 2011). Theoretically, a strong warming in winter could impede the fulfillment of the chilling requirement and thus lead to delays in the spring onset of growth (Nordli et al., 2008; Yu et al., 2010). For example, Yu et al. (2010) found that the shortening of the growing period across Tibetan Plateau meadow and steppe zones after the mid-1990 s was closely related to insufficient winter chilling. However, our result of a shift to an earlier onset of spring greening indicated that the winter climatic conditions under current warming extremes can still meet the chilling requirement; conversely, the increase in winter temperature has not yet reached a turning point leading to a delay in spring resumption of growth (Fig. S4). This finding suggested that the AM plants may have a relatively low chilling requirement. Further, warm winters may have also decreased the risk of freezing injury to the sensitive growing tissues of AM plants; this was shown at high altitudes, where frost damage restricted the growth of several woody and perennial herbaceous species (Inouye, 2008). Changes in SOS observed in this study suggested that recent extremely high temperatures may not exert a negative impact on spring green-up of AM plants, but further studies will be needed to determine whether such a response can persist in case of continued warming.

In arid ecosystems, shifts in the timing, frequency, and amount of precipitation also acted as important regulators of spring phenological responses to climatic warming (Jenerette et al., 2010). We found a significant influence of climatic extremes associated with precipitation on spring green-up of AM plants. Preseason droughts significantly decreased soil moisture content, and predisposed the shallow-rooted mountainous plants to water stress, resulting in delays in spring phenology. Conversely, larger amounts of preseason precipitation would reduce the risk of droughts and effectively increase soil water availability, promoting vegetation to maximize the thermal benefit (Shen et al., 2015). Within the QLMs, a steady decline in hydroclimatic sensitivity of SOS was detected when vegetation distribution shifted upward in elevation (Fig. 5). Such an underlying trend demonstrates the overall response of all plants with overlapping distribution, which is often complicated by different sensitivities among vegetation types. A unique finding of this study was that the sensitivity to drought peaked in the shrubland ecosystem at medium elevations, instead of in the low-altitude forests or steppes that are more water-limited (Fig. 4). This was not expected, as biomes at lower elevations, with less rainfall and higher temperatures, were thought to experience greater water stress and sensitivity to hydroclimatic variations than biomes at higher elevations, typically exhibiting more rainfall and lower temperatures (Linares et al., 2012; Butz et al., 2017). An example of a water-use pattern was reported for *Abies pinsapo* in European mountains; due to a strong water deficit, low-elevation trees generally had lower predawn xylem water potentials and earlier partial stomatal closure than observed for high elevation trees (Linares et al., 2012). However, Ma et al. (2015) recently found a skewed distribution of hydroclimatic sensitivity to aridity across a large geographical area in southeastern Australia, with semiarid ecosystems, but not arid biomes, being most sensitive to severe droughts. Our results were similar to those of Ma et al.'s (2015), even though this study reflected an altitudinal pattern while their study was based on a horizontal gradient.

This unique pattern of the impact of hydroclimatic variability on phenology is most probably associated with the physical environment of different altitudes and plant adaptability. In low-elevation forest biomes, extensive soil organic content maintains greater water holding capacity than in biomes with low soil organic matter contents. Thus, relatively high water content remains in forest subsoil, even on dry days or in drought periods (Yang et al., 2017). Additionally, AM forests are dominated by evergreen conifer species (Du et al., 2014), which develop drought-adapted strategies including a more efficient use of scattered rainfalls than is observed for deciduous species (Swidrak et al., 2013). In comparison, low water retention in shrubland ecosystems above the tree line is notable because subalpine shrubs commonly occupy steep inclines with thin sola and high soil porosity (He et al., 2015). The elevation-related precipitation amounts may not buffer

against water deficits caused by droughts. Shrubland ecosystem lacks adaptability to extreme precipitation events, and this contributes to its peak hydroclimatic sensitivity. Our findings suggest that an increase in the frequency of heavy rainfall and severe drought will lead to significant impacts on shrubland ecosystem, and this biome should be the focus of future work.

Climate projections indicate that the probability of coinciding multiple extreme events (e.g. striking warming with severe drought) may be greater than that of a single event (Sillmann and Roeckner, 2008). This could pose a major threat to terrestrial ecosystem function. It is, however, less clear how plant species respond to the superimposed effect of extreme climatic events. Our results revealed a significant advancement in the spring onset of growth in the AM ecosystems in response to recent abnormal warming and increased wetness, both of which are predicted to be more frequent in China in the future (Zhang et al., 2006). The observed changes in phenology may be an indication of greater rates of photosynthesis and larger production of biomass than is possible under normal climate conditions (Polgar and Primack, 2011). Ecosystem sensitivity was at roughly the same level for different land cover types (Fig. 4 and 5) although ecosystem responses to single extreme climatic events (extreme warming or heavy rainfall) were quite different. The combined influence of extreme warming and precipitation may involve synergistic mechanisms acting in an intricate way. We propose that these mechanisms are significant for an increased understanding of how AM ecosystems are and will be influenced by climate change.

5. Conclusions

This study of the impacts of recent extreme climatic events revealed strong responses of phenology in AM plants. The evidence of a warming-induced SOS advancement following a sharp rise in spring and winter temperatures suggests that AM plants may have relatively low chilling requirement for dormancy release. Recent warming may also have decreased the risk of freezing-induced stress during mid-winter. Contrary to the positive response to warming, spring phenology exhibited a widespread delay of growth during the drought year, with different land cover types displaying divergent sensitivities. The peak sensitivity of subalpine shrubs indicated that this ecosystem was most susceptible to hydroclimatic extremes, highlighting the great importance of this biome. Our study also provided initial evidence for phenological responses to coinciding multiple climatic extremes, which suggested that the combined influence of individual climatic extremes will be far from additive. Currently, it is still not clear how multiple climatic extremes synergistically affect the seasonal course of vegetation activity, representing an urgent need for further investigation.

Acknowledgements

This work was supported by the National Natural Science Foundation of China (No. 41522102 and 41601051) and Funds for Creative Research Groups of China (No. 41621001).

Appendix A. Supplementary data

Supplementary material related to this article can be found, in the online version, at doi:https://doi.org/10.1016/j.agrformet.2018.05.022.

References

Badeck, F.W., Bondeau, A., Böttcher, K., Doktor, D., Lucht, W., Schaber, J., Sitch, S., 2004. Responses of spring phenology to climate change. New Phytol. 162 (2), 295–309.
Beniston, M., 2003. Climatic change in mountain regions: a review of possible impacts. Clim. Change 59 (1), 5–31.
Bourque, C.P.A., Mir, M.A., 2012. Seasonal snow cover in the qilian mountains of Northwest China: its dependence on oasis seasonal evolution and lowland production of water vapour. J. Hydrol. 454, 141–151.
Butt, N., Seabrook, L., Maron, M., Law, B.S., Dawson, T.P., Syktus, J., McAlpine, C.A., 2015. Cascading effects of climate extremes on vertebrate fauna through changes to low-latitude tree flowering and fruiting phenology. Global Change Biol. 21 (9), 3267–3277.
Butz, P., Raffelsbauer, V., Graefe, S., Peters, T., Cueva, E., Hölscher, D., Bräuning, A., 2017. Tree responses to moisture fluctuations in a neotropical dry forest as potential climate change indicators. Ecol. Indic. 83, 559–571.
Crabbe, R.A., Dash, J., Rodriguez-Galiano, V.F., Janous, D., Pavelka, M., Marek, M.V., 2016. Extreme warm temperatures alter forest phenology and productivity in Europe. Sci. Total Environ. 563, 486–495.
Crimmins, T.M., Crimmins, M.A., David Bertelsen, C., 2010. Complex responses to climate drivers in onset of spring flowering across a semi-arid elevation gradient. J. Ecol. 98 (5), 1042–1051.
Delbart, N., Le Toan, T., Kergoat, L., Fedotova, V., 2006. Remote sensing of spring phenology in boreal regions: a free of snow-effect method using NOAA-AVHRR and SPOT-VGT data (1982–2004). Remote Sens. Environ. 101 (1), 52–62.
Diaz, H.F., Grosjean, M., Graumlich, L., 2003. Climate variability and change in high elevation regions: past, present and future. Clim. Change 59 (1), 1–4.
Dorji, T., Totland, Ø., Moe, S.R., Hopping, K.A., Pan, J., Klein, J.A., 2013. Plant functional traits mediate reproductive phenology and success in response to experimental warming and snow addition in Tibet. Global Change Biol. 19, 459–472.
Du, J., He, Z.B., Yang, J.J., Chen, L.F., Zhu, X., 2014. Detecting the effects of climate change on canopy phenology in coniferous forests in semi-arid mountain regions of China. Int. J. Remote Sens. 35, 6490–6507.
Ghalambor, C.K., Mckay, J.K., Carroll, S.P., Reznick, D.N., 2007. Adaptive versus non-adaptive phenotypic plasticity and the potential for contemporary adaptation in new environments. Funct. Ecol. 21, 394–407.
Ghelardini, L., Santini, A., Black-Samuelsson, S., Myking, T., Falusi, M., 2010. Bud dormancy release in elm (Ulmus spp.) Clones – a case study of photoperiod and temperature responses. Tree Physiol. 30, 264–274.
He, Z.B., Du, J., Zhao, W.Z., Yang, J.J., Chen, L.F., Zhu, X., Chang, X.X., Liu, H., 2015. Assessing temperature sensitivity of subalpine shrub phenology in semi-arid mountain regions of China. Agric. For. Meteorol. 213, 42–52.
Heyder, U., Schaphoff, S., Gerten, D., Lucht, W., 2011. Risk of severe climate change impact on the terrestrial biosphere. Environ. Res. Lett. 6 (3), 034036.
Inouye, D.W., 2008. Effects of climate change on phenology, frost damage, and floral abundance of montane wildflowers. Ecology 89, 353–362.
Jenerette, G.D., Scott, R.L., Huete, A., 2010. Functional differences between summer and winter season rain assessed with MODIS-derived phenology in a semi-arid region. J. Veg. Sci. 21, 16–30.
Jeong, S.J., Ho, C.H., Gim, H.J., Brown, M.E., 2011. Phenology shifts at Start vs. end of growing season in temperate vegetation over the Northern Hemisphere for the period 1982–2008. Global Change Biol. (17), 2385–2399.
Jiang, Y.Y., Ming, J., Ma, P.L., Wang, P.L., Du, Z.C., 2016. Variation in the snow cover on the Qilian Mountains and its causes in the early 21st century. Geomat. Nat. Haz. Risk 7 (6), 1824–1834.
Julitta, T., Cremonese, E., Migliavacca, M., Colombo, R., Galvagno, M., Siniscalco, C., Rossini, M., Fava, F., Cogliai, S., di Cella, U.M., Menzel, A., 2014. Using digital camera images to analyze snowmelt and phenology of a subalpine grassland. Agric. For. Meteorol. 1 (98), 116–125.
Kross, A., Fernandes, R., Seaquist, J., Beaubien, E., 2011. The effect of the temporal resolution of NDVI data on season onset dates and trends across Canadian broadleaf forests. Remote Sens. Environ. 1 (15), 1564–1575.
Lesica, P., Kittelson, P.M., 2010. Precipitation and temperature are associated with advanced flowering phenology in a semi-arid grassland. J. Arid Environ. 74 (9), 1013–1017.
Lin, P., He, Z., Du, J., Chen, L., Zhu, X., Li, J., 2017. Recent changes in daily climate extremes in an arid mountain region, a case study in northwestern China's Qilian Mountains. Sci. Rep. 7.
Linares, J.C., Covelo, F., Carreira, J.A., Merino, J.Á., 2012. Phenological and water-use patterns underlying maximum growing season length at the highest elevations: implications under climate change. Tree Physiol. 32 (2), 161–170.
Luedeling, E., Gassner, A., 2012. Partial least squares regression for analyzing walnut phenology in California. Agric. For. Meteorol. 1 (58), 43–52.
Ma, X., Huete, A., Moran, S., Ponce-Campos, G., Eamus, D., 2015. Abrupt shifts in phenology and vegetation productivity under climate extremes. J. Geophys. Res. - Biogeo. 120 (10), 2036–2052.
Menzel, A., Seifert, H., Estrella, N., 2011. Effects of recent warm and cold spells on European plant phenology. Int. J. Biometeorol. 55 (6), 921–932.
Nemani, R.R., Keeling, C.D., Hashimoto, H., Jolly, W.M., Piper, S.C., Tucker, C.J., Running, S.W., 2003. Climate-driven increases in global terrestrial net primary production from 1982 to 1999. Science 300 (5625), 1560–1563.
Nogués-Bravo, D., Araújo, M.B., Errea, M.P., Martinez-Rica, J.P., 2007. Exposure of global mountain systems to climate warming during the 21st century. Global Environ. Chang. 17 (3), 420–428.
Nordli, O., Wielgolaski, F.E., Bakken, A.K., Hjeltnes, S.H., Mage, F., Sivle, A., Skre, O., 2008. Regional trends for bud burst and flowering of woody plants in Norway as related to climate change. Int. J. Biometeorol. 52, 625–639.
Parmesan, C., Yohe, G., 2003. A globally coherent fingerprint of climate change impacts across natural systems. Nature 421 (6918), 37.
Peng, S.S., Piao, S.L., Ciais, P., Fang, J.Y., Wang, X.H., 2010. Change in winter snow depth and its impacts on vegetation in China. Global Change Biol. 16 (11), 3004–3013.
Peñuelas, J., Filella, I., 2009. Phenology feedbacks on climate change. Science 324 (5929), 887–888.
Pettorelli, N., Vik, J.O., Mysterud, A., Gaillard, J.M., Tucker, C.J., Stenseth, N.C., 2005.

Using the satellite-derived NDVI to assess ecological responses to environmental change. Trends Ecol. Evol. (20), 503–510.
Polgar, C.A., Primack, R.B., 2011. Leaf-out phenology of temperate woody plants: from trees to ecosystems. New Phytol. 191, 926–941.
Prevéy, J.S., Seastedt, T.R., 2014. Seasonality of precipitation interacts with exotic species to alter composition and phenology of a semi-arid grassland. J. Ecol. 102 (6), 1549–1561.
Rich, P.M., Breshears, D.D., White, A.B., 2008. Phenology of mixed woody–herbaceous ecosystems following extreme events: net and differential responses. Ecology 89 (2), 342–352.
Richardson, A.D., Keenan, T.F., Migliavacca, M., Ryu, Y., Sonnentag, O., Toomey, M., 2013. Climate change, phenology, and phenological control of vegetation feedbacks to the climate system. Agric. For. Meteorol. 169, 156–173.
Shen, M.G., Piao, S.L., Cong, N., Zhang, G.X., Jassens, I.A., 2015. Precipitation impacts on vegetation spring phenology on the Tibetan Plateau. Global Change Biol. 21 (10), 3647–3656.
Siegmund, J.F., Wiedermann, M., Donges, J.F., Donner, R.V., 2016. Impact of temperature and precipitation extremes on the flowering dates of four German wildlife shrub species. Biogeosciences 13 (19), 5541.
Sillmann, J., Roeckner, E., 2008. Indices for extreme events in projections of anthropogenic climate change. Clim. Change 86 (1–2), 83–104.
Swidrak, I., Schuster, R., Oberhuber, W., 2013. Comparing growth phenology of co-occurring deciduous and evergreen conifers exposed to drought. Flora 208 (10), 609–617.
Thuiller, W., Lavorel, S., Araújo, M.B., Sykes, M.T., Prentice, I.C., 2005. Climate change threats to plant diversity in Europe. Proc. Natl. Acad. Sci. U. S. A. 102 (23), 8245–8250.
Walther, G.R., Post, E., Convey, P., Menzel, A., Parmesan, C., Beebee, T.J., Fromentin, J.M., Hoegh-Guldberg, O., Bairlein, F., 2002. Ecological responses to recent climate change. Nature 416 (6879), 389–395.
Wang, T., Peng, S.S., Lin, X., Chang, J.F., 2013. Declining snow cover may affect spring phenological trend on the Tibetan Plateau. Proc. Natl. Acad. Sci. U. S. A. 110 (31), E2854–E2855.
Yang, J., He, Z., Du, J., Chen, L., Zhu, X., Lin, P., Li, J., 2017. Soil water variability as a function of precipitation, temperature, and vegetation: a case study in the semiarid mountain region of China. Environ. Earth Sci. 76 (5), 206.
Yu, H., Luedeling, E., Xu, J., 2010. Winter and spring warming result in delayed spring phenology on the tibetan plateau. Proc. Natl. Acad. Sci. U. S. A. 107 (51), 22151–22156.
Zhang, S., Tao, F., 2013. Modeling the response of rice phenology to climate change and variability in different climatic zones: comparisons of five models. Eur. J. Agron. 45, 165–176.
Zhang, X.Y., Friedl, M.A., Schaaf, C.B., Strahler, A.H., 2004. Climate controls on vegetation phenological patterns in northern mid-and high latitudes inferred from MODIS data. Global Change Biol. 10 (7), 1133–1145.
Zhang, Y., Xu, Y., Dong, W., Cao, L., Sparrow, M., 2006. A future climate scenario of regional changes in extreme climate events over China using the PRECIS climate model. Geophys. Res. Lett. 33 (24).
Zhang, G.L., Zhang, Y.J., Dong, J.W., Xiao, X.M., 2013. Green-up dates in the Tibetan Plateau have continuously advanced from 1982 to 2011. Proc. Natl. Acad. Sci. U. S. A. 110 (11), 4309–4314.
Zhou, J.H., Cai, W.T., Qin, Y., Lai, L.M., Guan, T.Y., Zhang, X.L., Jiang, L.H., Du, H., Yang, D.W., Cong, Z.T., Zheng, Y.R., 2016. Alpine vegetation phenology dynamic over 16 years and its covariation with climate in a semi-arid region of China. Sci. Total Environ. 572, 119–128.